Current-voltage characteristics of two-dimensional vortex-glass models

R. A. Hyman
Department of Physics, Indiana University, Bloomington, Indiana 47405

Mats Wallin
Department of Theoretical Physics Royal Institute of Technology, S-100 44 Stockholm, Sweden

M. P. A. Fisher
Institute for Theoretical Physics, University of California, Santa Barbara, California 93106

S. M. Girvin
Department of Physics, Indiana University, Bloomington, Indiana 47405

A. P. Young
Department of Physics, University of California, Santa Cruz, California 95064
(Received 13 October 1994)

We have performed Monte Carlo simulations to determine current-voltage characteristics of two vortex-glass models in two dimensions. Our results confirm earlier studies which concluded that there is a zero-temperature transition. Additionally we find that, as the temperature approaches zero, the linear resistance vanishes exponentially, and the current scale J_{nl} where nonlinearities appear in the current-voltage characteristics, varies roughly as T^3. This result is quite different from the prediction of conventional flux creep theory in which $J_{nl} \sim T$. The results for the two models agree quite well with each other, and also agree fairly well with recent experiments on very thin films of Y-Ba-Cu-O.

I. INTRODUCTION

In a magnetic field, the effects of fluctuations and defects in high-T_c superconductors are particularly strong.[1] In fact, much of the H-T phase diagram of high-T_c materials is occupied by a "vortex-liquid" regime which is not present in the mean-field phase diagram. When a current is applied to a superconductor in the vortex-liquid regime, the resistance is not zero because flux lines move under the action of a Lorentz force and produce a Josephson voltage.[2] An important question, is whether at lower temperature, defects can collectively pin flux lines so that they have no linear response to the Lorentz force, thus implying a vanishing linear resistance. In the presence of defects, there is no long-range order in the positions of vortices.[3] Nonetheless, a transition to a state with vanishing linear resistance may occur.[4] Such a state is called the vortex glass.

While there is theoretical[5,6] and experimental[7] evidence for a finite vortex-glass transition temperature T_c in bulk superconductors, several simulations[8,6] have clearly shown that $T_c = 0$ in two-dimensional systems, and rigorous analytic arguments[9] have established that there is no vortex-glass order at finite temperature in two dimensions.

Recent work[10] has shown that inclusion of gauge-field fluctuations (i.e., screening) changes the universality class, but the transition temperature is still zero in two dimensions. Even though $T_c = 0$, there are observable consequences at finite temperatures because the correlation length diverges as the temperature approaches zero. We shall discuss these consequences in detail. In contrast, a different simulation of the nonlinear current-voltage characteristics of the gauge glass in two dimensions found evidence for a finite T_c.[11] However, behavior consistent with $T_c = 0$ has recently been observed[12] in experiments on 16-Å films of Y-Ba-Cu-O.

Although the experiments[12] on two-dimensional samples are in quite good agreement with theory, they measure different quantities from what has been calculated and a scaling hypothesis is needed to make a comparison. The experiments determined current-voltage (I-V) characteristics, while the simulations investigated the size dependence of the rigidity of the system with respect to a twist in the phase of the condensate. It therefore seems worthwhile to make a *direct* comparison of simulation and experiment by calculating I-V characteristics from simulations of two-dimensional systems. As an additional benefit, we study *two* models which are somewhat different microscopically: the gauge glass, defined in Eq. (1) below, which has effectively *random* fluxes penetrating the sheet; and a more realistic model, defined in Eq. (14) below, which has a net *uniform* field penetrating the sheet and a random pinning potential for the vortices. We find that universal properties are the same for these two models. Since the gauge glass has been extensively used for numerical studies of the vortex-glass transition, it is reassuring that it gives the same results as a model with a net field, at least in two dimensions.

II. THE MODELS

The first model that we study is the gauge glass,[5,6,8] whose Hamiltonian is

$$\mathcal{H}_{\rm gg} = -\sum_{\langle i,j\rangle} \cos(\phi_i - \phi_j - A_{ij}). \tag{1}$$

The phase of the condensate ϕ_i is defined on each site i of a square lattice, with $N = L^2$ sites. The sum is over all nearest-neighbor pairs on the lattice. The effects of the external magnetic field and the defects are both represented by the quenched vector potentials A_{ij} which are taken to be independent random variables with a uniform distribution between 0 and 2π.

To compute the I-V characteristics we need to incorporate dynamics into the model. The standard way of doing this is to view the model as a set of coupled Josephson junctions.[13–15] Josephson's and Kirchoff's equations for the current are then

$$I_{ij} = \frac{V_{ij}}{R_0} + I_c \sin(\phi_i - \phi_j - A_{ij}) + \eta_{ij}(t), \tag{2}$$

$$V_{ij} = \frac{\hbar}{2e}\frac{d}{dt}(\phi_i - \phi_j), \tag{3}$$

$$\sum_j I_{ij} = I_{i:\rm ext}, \tag{4}$$

where i and j are nearest-neighbor pairs. Equation (2) expresses the sum of the current from site i to neighboring site j as the sum of a resistive current given by V_{ij}/R_0, a Josephson current, and a Langevin current noise source $\eta_{ij}(t)$. I_c is the maximum Josephson current of the nearest-neighbor pair, and R_0 is the shunt resistance of the pair. The thermal noise has a Gaussian distribution with the following properties:

$$\langle \eta_{ij}(t)\rangle = 0, \tag{5}$$

$$\langle \eta_{ij}(t)\eta_{kl}(t')\rangle = \frac{2k_BT}{R_0}\delta_{ij,kl}\delta(t-t'), \tag{6}$$

which ensures that the system comes to thermal equilibrium at temperature T. Equation (3) is the Josephson relation connecting the voltage V_{ij} with the time derivative of the phase difference $\phi_i - \phi_j$. Equation (4) is Kirchoff's law expressing current conservation at site i. $I_{i:\rm ext}$ is the external current at site i. This is zero except for sites on the top row where an external current $J \equiv I/L$, is fed in, and sites on the bottom row where the same current is extracted. The *total* current through the sample is then I. We take the system to be a cylinder with periodic boundary conditions in the direction perpendicular to the current. The average voltage drop along the system V is given by

$$V = \frac{1}{L^2}\frac{\hbar}{2e}\sum_{i\in\rm bottom}\sum_{j\in\rm top}\frac{d}{dt}\langle\phi_i - \phi_j\rangle, \tag{7}$$

where the brackets $\langle\cdots\rangle$ denote a time average. The average electric field is then $E = V/L$. For this model we work in units where $\hbar/(2e) = R_0 = I_c = 1$. Throughout the paper we also set Boltzmann's constant to be unity. Equations (2)–(4) are solved by the standard matrix inversion method, described in detail in Ref. 13. The equations of motion are integrated using a first-order approximation with a time step of $\delta\tau = 0.05\tau$, where $\tau = \hbar/(2eR_0I_c)$ is the basic unit of time (which is set equal to unity). The scale of τ is the typical time for a neighboring pair of sites to accumulate a relative phase of order unity.

We have also studied an equivalent form for the gauge glass written in terms of vortices. In contrast to the phase representation of the model discussed above, it is convenient to impose periodic boundary conditions on a torus. To obtain the gauge-glass model in the vortex representation we replace the cosine in Eq. (1) by the periodic Gaussian (Villain) function,[16] and perform standard manipulations[16,17] which yield

$$\mathcal{H}^V_{\rm gg} = -\frac{1}{2}\sum_{i,j}[n_i - b_i]G(i-j)[n_j - b_j], \tag{8}$$

where the $\{n_i\}$ are integer valued vortex "charges." The vortices sit on the sites of the dual lattice, which lie in the centers of the squares of the original lattice. The magnetic fluxes b_i are the lattice curl of the vector potential. They are given by the product of $1/2\pi$ and the directed sum of the quenched vector potentials on the links of the original lattice which surround the site i of the dual lattice. The periodic boundary conditions enforce the constraint $\sum_i b_i = 0$, and the integration over the zero wave-vector piece of the phase variable enforces the constraint $\sum_j n_j - b_j = 0$. Thus we have a "charge neutrality" constraint $\sum_i n_i = 0$. $G(i-j)$ is the vortex interaction

$$G(i-j) = \left(\frac{2\pi}{L}\right)^2 \sum_{\mathbf{k}\neq 0}\frac{1 - \exp[i\mathbf{k}\cdot(\mathbf{r_i} - \mathbf{r_j})]}{4 - 2\cos k_x - 2\cos k_y}. \tag{9}$$

At large distance, $G(i-j) \to 2\pi \ln|\mathbf{r_i} - \mathbf{r_j}|$.

We study the I-V characteristics of this vortex model by using Monte Carlo dynamics. That is, we equate Monte Carlo time and real time, an approximation which is expected to be good in the limit of overdamped dynamics and which has proven reasonable in other simulations.[18] Choosing a nearest-neighbor pair (i,j) at random, we try to increase n_i by 1 and decrease n_j by 1, thus transferring a unit vortex from j to i. Following the "heat bath" algorithm, if the change in energy is ΔE, the move is accepted with the probability $1/[1+\exp(\beta\Delta E)]$. An applied current density J gives a Lorentz force of $Jh/2e$ on a unit vortex. The Lorentz force can be incorporated into the Monte Carlo moves[18] by adding to ΔE an amount $Jh/(2e)$ if the vortex moves in the direction opposite to the Lorentz force, subtracting this amount if it moves in the same direction, and making no change in ΔE if it moves in a perpendicular direction. Biasing the moves in this way takes the system out of equilibrium and causes a net flux of vortices in a direction perpendicular to the current. This then generates a voltage V, where

$$V = \frac{h}{2e}\langle I^V(t)\rangle, \tag{10}$$

with

$$I^V(t) = \frac{1}{L\Delta t}\sum_i \Delta Q_i^V(t), \tag{11}$$

where $I^V(t)$ is the vortex current. Here t denotes a Monte Carlo time (incremented by Δt after each attempted move), and $\Delta Q_i^V(t) = 1$ if a vortex at site i moves one lattice spacing in the direction of the Lorentz force at time t, $\Delta Q_i^V(t) = -1$ if the vortex moves in the direction opposite to the Lorentz force, and $\Delta Q_i^V(t) = 0$ otherwise. We set $\Delta t = 1/4N$ so that an attempt is made to move each vortex once in each direction, on average, per unit time. We shall use units where $h/2e = 1$ when dealing with vortex models.

The linear resistance can also be obtained from the Kubo formula for fluctuations in the voltage in the absence of any net current. The Kubo formula is exact for discrete time Monte Carlo dynamics provided the sum over time is made symmetrical about $t = 0$,[19] i.e.,

$$R_{\rm lin} = \frac{1}{2T}\sum_{t=-\infty}^{\infty}\Delta t\ \langle V(t)V(0)\rangle, \tag{12}$$

which, in our units, can be expressed in terms of the vortex current as

$$R_{\rm lin} = \frac{1}{2T}\sum_{t=-\infty}^{\infty}\Delta t\ \langle I^V(t)I^V(0)\rangle. \tag{13}$$

Using Monte Carlo dynamics should be a good approximation near a critical point, where the vortex motion is slow and overdamped. However, because of discretization of time, and the fact that the fastest a vortex can move is one lattice spacing per time step, it is not very satisfactory for large currents or high temperatures. For example, at high temperatures with no bias current, a vortex moves in the $\pm$ x direction with probability 1/4. From Eq. (13), the resistance is then given by $R_{\rm lin} = 1/(2T)$ and tends to zero, which is unphysical.

The gauge glass represents a system with *random* fluxes penetrating the film but with zero net field. The gauge glass is a convenient model to study but it should be verified that it is in the same universality class as experimental systems which have a *net* uniform field penetrating the film and a random pinning potential for the vortices. We have therefore also studied a random pinning model with the following Hamiltonian,

$$\mathcal{H}_{\rm rp} = -\frac{1}{2}\sum_{i,j}[n_i - f]G(i-j)[n_j - f] - \sum_i v(i)n_i^2, \tag{14}$$

where the n_i are restricted to the values 0 and ± 1, $G(i-j)$ is given by Eq. (9), and $v(i)$ is a random pinning potential, uniformly distributed in the interval $-\Delta < v(i) < \Delta$. We set $\Delta = \pi$. We also fix the net filling, f [$\equiv (1/N)\sum_i n_i$], which effectively determines the magnetic field, to be 1/4. [Note that because of the periodic boundary conditions and the fact that the zero wave-vector part of G has been removed, it is not actually necessary to include the f terms in Eq. (14).] We obtain I-V characteristics from Monte Carlo dynamics. At each Monte Carlo time we try to insert a $(+1,-1)$ pair at a randomly chosen pair of sites i and j. The analysis is then precisely the same as described above for the vortex representation of the gauge glass.

III. SCALING THEORY

To analyze the results it is necessary to understand how the I-V characteristics vary in the vicinity of a second-order phase transition. A detailed scaling theory has been developed[1] and we now summarize the results for the case of a zero-temperature transition, where the correlation length diverges as

$$\xi \sim T^{-\nu}, \tag{15}$$

and the relaxation time τ also diverges. Normally one defines a dynamic exponent z by $\tau \sim \xi^z$, but since the transition is at zero temperature, the relaxation has an activated form and diverges exponentially as the temperature approaches zero. Formally this corresponds to $z = \infty$.

The vector potential $\mathbf{A}$ enters the Hamiltonian in Eq. (1) in the dimensionless form $A_{ij} \sim \int_j^i \mathbf{A}(\mathbf{r})\cdot d\mathbf{r}$. Therefore $\mathbf{A}$ scales as $1/\xi$. The electric field is given by $\mathbf{E} = -\partial_t\mathbf{A}$ and so scales as $1/(\xi\tau)$. $\mathbf{J}\cdot\mathbf{E}$, the energy dissipated per unit volume per unit time, scales like $k_BT/(\xi^d\tau)$. Therefore J scales like k_BT/ξ^{d-1}. It is important to keep the factor of T because $T_c = 0$. Combining these results we obtain (for $k_B = 1$)

$$T\frac{E}{J}\frac{\tau}{\xi^{d-2}} = g\left(\frac{J\xi^{d-1}}{T}\right), \tag{16}$$

where g is a scaling function. In two dimensions with $T_c = 0$ this becomes

$$T\tau\frac{E}{J} = g\left(\frac{J}{T^{1+\nu}}\right). \tag{17}$$

From Eq. (17) one sees that the characteristic current scale J_{nl} at which nonlinear behavior sets in, varies with T as

$$J_{nl} \sim T^{1+\nu}. \tag{18}$$

The linear resistance is

$$R_{\rm lin} = \lim_{J\to 0}\frac{E}{J}, \tag{19}$$

and $g(0)$ must be a constant, which we take to be unity, so we can write

$$\frac{E}{JR_{\rm lin}} = g\left(\frac{J}{T^{\nu+1}}\right), \tag{20}$$

and

$$TR_{\rm lin} = \frac{1}{\tau} = A \exp\left[-\Delta E(T)/T\right], \tag{21}$$

where $\Delta E(T)$ is the typical barrier that a vortex has to cross to move a distance ξ. One conventionally defines a barrier exponent ψ by $\Delta E \sim \xi^{\psi} \sim T^{-\psi\nu}$ in terms of which

$$TR_{\rm lin} \sim \exp\left(-C/T^{1+\psi\nu}\right). \tag{22}$$

It has been suggested[1] that ψ may be zero in two dimensions, leading to barriers which are either finite as the temperature approaches zero or diverge logarithmically. In the latter case the linear resistance would vary as $\exp\left(-C|\ln(T)|^{\mu}/T\right)$, where μ is another exponent.

In Eq. (21), the linear resistance is seen to vanish exponentially as the temperature approaches zero. In these circumstances it is generally more difficult to estimate the form of possible power-law prefactors than the form of the leading exponential dependence. We have incorporated a factor of T on the left-hand side of Eq. (21) because it emerged naturally from the scaling ansatz. This factor of T also looks reasonable when compared with the Kubo formula, Eq. (13), since it is $TR_{\rm lin}$ which is given by the voltage fluctuations. However, it is possible that additional factors of T could be present in the scaling region.

In a finite system, the I-V characteristics will also depend on the size of the system when the bulk correlation length ξ becomes comparable with L. According to finite-size scaling[20] only the ratio L/ξ is important. Therefore, from Eq. (15), one can generalize Eq. (20) to

$$\frac{E}{JR_{\rm lin}} = \tilde{g}\left(\frac{J}{T^{1+\nu}},\ L^{1/\nu}T\right). \tag{23}$$

The nonlinear behavior in the finite-size regime, described by Eq. (23), is rather complicated because it involves a function of two variables. Consequently, we have studied nonlinear behavior either in the range where finite-size corrections are negligible or, having already determined ν, choose L and T such that the second argument $L^{1/\nu}T$ is constant.

IV. RESULTS

In Fig. 1 we show some of the experimental data of Dekker *et al.*[12] on 16-Å films of Y-Ba-Cu-O. For small current densities, the data is flat, indicating Ohm's law, with a linear resistivity which decreases rapidly with decreasing temperature. As J is increased the data starts to curve upwards, indicating nonlinear response. The current scale J_{nl} at which nonlinear behavior sets in, is also seen to decrease with decreasing temperature. Analyzing all their data, Dekker *et al.* find that the linear resistivity varies as

$$R_{\rm lin} \sim \exp(-C/T^{p}) \tag{24}$$

with $p \simeq 0.6$. This variation, which is less rapid than an Arrhenius form $p = 1$ is difficult to understand from the classical models which we study here. It may therefore indicate that quantum tunneling of vortices is important at the lowest temperatures. On the other hand, J_{nl} is found to vary with T as T^3, which, from Eq. (18) implies $\nu \simeq 2$. This result is in agreement with our simulations and earlier studies[8,6] of the gauge glass.

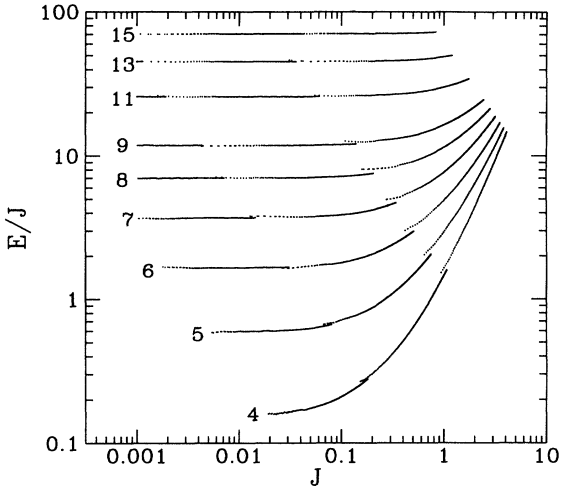

FIG. 1. Plot of some of the experimental data, at a field of 0.5 T, on 16-Å films of Y-Ba-Cu-O from Ref. 12. The numbers denote the temperatures, in kelvin, at which the different data sets were taken.

We next discuss our numerical results for the I-V characteristics of the gauge glass in the vortex representation. Data for T times the linear resistance against $1/T$ is shown in Fig. 2 on a log-linear plot. A simple Arrhenius form, i.e., a temperature-independent barrier height ΔE would correspond to a straight line. In fact for the largest size, the data is very close to a straight line indicating that the barrier exponent ψ in Eq. (22) is zero or nearly

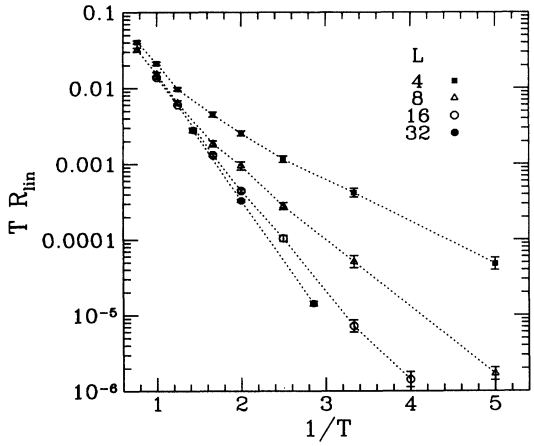

FIG. 2. Plot of the product T and linear resistance, on a logarithmic scale, against $1/T$ for different sizes of gauge glass in the vortex representation. The data for the largest size, $L = 32$, is well approximated by a straight line, indicating a temperature-independent barrier height, i.e., Arrhenius behavior.

zero. These results are consistent with the suggestion[1] of a logarithmically increasing barrier, but this weak dependence will be difficult to see on data which are over a modest range of temperatures in finite-size systems.

Data for the nonlinear response at finite J is shown in Fig. 3. The data for the smallest current density J was actually obtained for $J = 0$ from the Kubo formula, Eq. (13). As in the experimental results in Fig. 1, the data follow Ohm's law at small J (where each data set is horizontal) with a linear resistance which decreases rapidly with temperature, as shown in more detail in Fig. 2. Deviations from Ohms law occur at a scale J_{nl} where the data start to curve upwards. J_{nl} decreases with decreasing temperature, as expected. From Fig. 2, finite-size effects appear quite small for $L = 16$ at $T = 0.5$ and 0.8. Similarly, assuming $\nu \approx 2$, the data for $L = 32$ in Fig. 2 at $T = 0.35$ should not be significantly affected by finite size effects. We have therefore analyzed the data in Fig. 3 according to the expected result for bulk behavior, Eq. (20). The scaling plot is shown in Fig. 4. The data scales reasonably well with $\nu = 1.8$ which is in quite good agreement with other estimates.[8,6] The values of $R_{\rm lin}$ in this plot were obtained from the Kubo formula.

Next we discuss the data obtained for the phase representation of the gauge glass. Results for the linear resistance are shown in Fig. 5. The data is consistent with an Arrhenius form for the largest sizes, as was found for the vortex representation (Fig. 2). Results for nonlinear current-voltage characteristics for the gauge glass in the phase representation are shown in Fig. 6. Unlike the vortex representation, which has discrete time and so a maximum vortex velocity, the dynamics of the phase representation use continuous time[21] and so can sensibly be

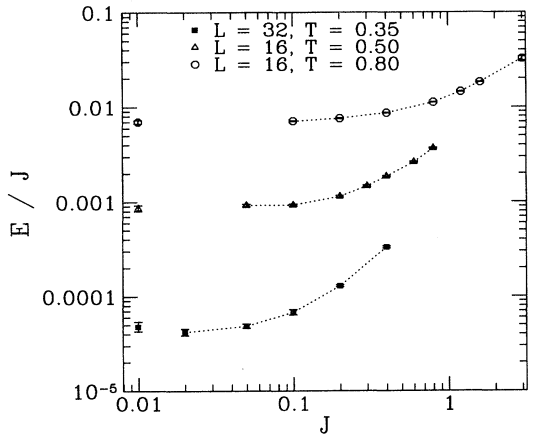

FIG. 3. Log-log plot of the nonlinear current-voltage characteristics of the gauge glass in the vortex representation. The data for the smallest current density J is actually for $J = 0$ and was obtained from the Kubo formula, Eq. (13). The data follow Ohm's law at small J (where each dataset is horizontal) with a linear resistance which decreases rapidly with temperature, as shown in more detail in Fig. 2. Deviations from Ohm's law, where the data start to curve, occur at a current scale J_{nl}, which decreases with decreasing temperature. Computations were not performed at extremely high currents outside the scaling regime, but the curves are expected to saturate as in Fig. 6.

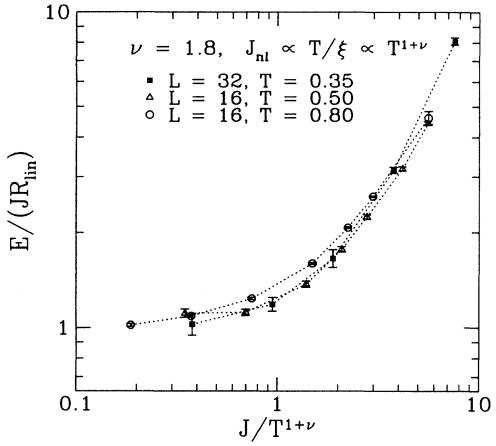

FIG. 4. Scaling plot of the data in Fig. 3, assuming that finite-size corrections are small and the scaling form expected for bulk behavior, Eq. (20), is appropriate. The value $\nu = 1.8$ obtained from this fit, is is reasonable agreement with other estimates.

applied for large values of J (and also high T). In Fig. 6 one clearly sees a "flux-flow" regime for large J, where the Lorentz force is sufficient to overcome pinning, and the only hindrance to vortex motion comes from friction. This leads to a resistance which is roughly independent of J and also only rather weakly dependent on temperature. For small J, however, the vortices are pinned by defects and move only by activation over barriers. The linear resistance in this "flux-creep" regime, is therefore much smaller than that observed for larger J and is also strongly temperature dependent.

We next describe our results for the random pinning potential model in Eq. (14). The linear resistance is shown in Fig. 7. As for the gauge glass, the data for the larger sizes seem to be tending towards an Arrhenius

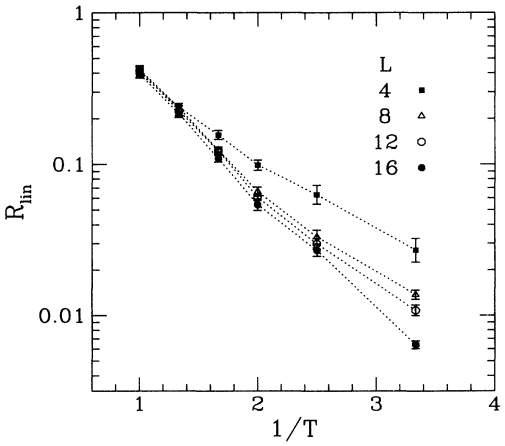

FIG. 5. Plot of the linear resistance, on a logarithmic scale, against $1/T$ for different sizes of gauge glass in the phase representation. The data for the largest size, $L = 16$, is fairly close to a straight line, indicating a temperature-independent barrier height, i.e., Arrhenius behavior. This is similar to the linear resistance data from the gauge-glass simulations in the vortex representation, Fig. 2.

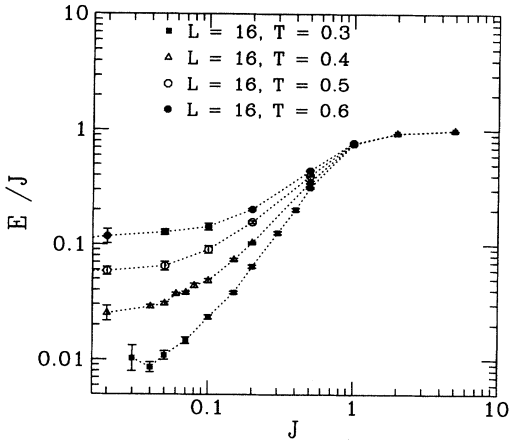

FIG. 6. Results for nonlinear current-voltage characteristics for the gauge glass in the phase representation. There is a flux-flow regime for large J, where the resistance is largely independent of J and T, and a flux-creep region at small J where the linear resistance is small and strongly temperature dependent. Deviations from the Ohm's law behavior at small J occur at a current scale J_{nl}, which decreases as T decreases.

behavior.

The nonlinear behavior of the random pinning potential model is shown in Fig. 8. As for the gauge-glass results in Fig. 6 there is a flux-flow regime for large J, and a flux-creep regime at small J where the linear resistance is small and strongly temperature dependent. Deviations from the Ohm's law behavior in the flux-creep regime occur at a current scale J_{nl}, which decreases as T decreases. For sufficiently large J, E will saturate, because there is a maximum vortex velocity when each vortex hops every

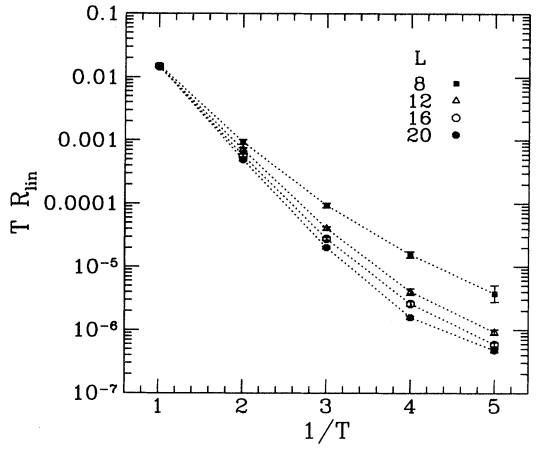

FIG. 7. Plot of the linear resistance, on a logarithmic scale, against $1/T$ for different sizes of the random pinning potential model in Eq. (14). The data for the largest sizes seems to be tending to a straight line, indicating a temperature-independent barrier height, i.e., Arrhenius behavior. This is similar to linear resistance data from the gauge–glass simulations, see Figs. 2 and 5.

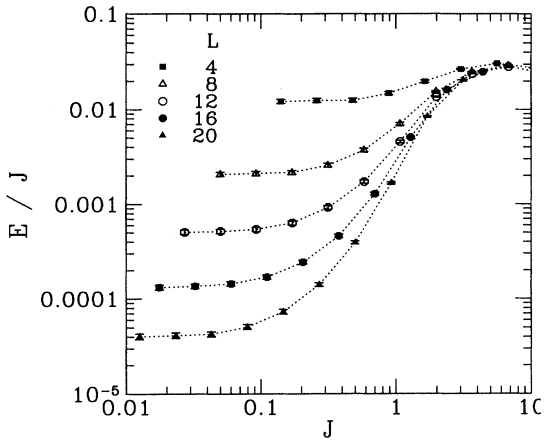

FIG. 8. Results for nonlinear current-voltage characteristics for the random pinning potential model in Eq. (14). For each size, L, the temperature has been chosen so that $LT^2 = 2$, in order to keep the second argument of the finite-size scaling function in Eq. (23) constant. The net filling, f ($\equiv (1/N)\sum_i n_i$), is equal to 1/4. As for the gauge-glass results presented in Fig. 6, there is a flux-flow regime for large J, and a flux-creep region at small J where the linear resistance is small and strongly temperature dependent. Deviations from the Ohm's law behavior in the flux-creep regime occur at a current scale J_{nl}, which decreases as T decreases.

step, so the ratio E/J will decrease. This (unphysical) behavior, which is just visible in the figure at the largest values of J, is caused by discretization of time in the Monte Carlo simulations. This discretization is, however, *not* expected to affect universal critical properties near the $T = 0$ critical point.

A scaling plot of the nonlinear I-V characteristics of the random pinning potential model is shown in Fig. 9. Since there are finite-size effects within the range of accessible sizes, we assume that $\nu \simeq 2$, and choose sizes and temperatures such that LT^2 is constant. In this way, the second argument in the scaling function in Eq. (23)

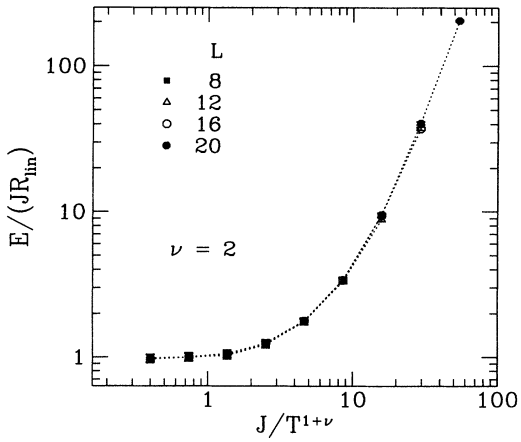

FIG. 9. Scaling plot of the nonlinear current-voltage characteristics of the random pinning potential model, assuming $\nu \simeq 2$, and choosing sizes and temperatures such that LT^2 is constant.

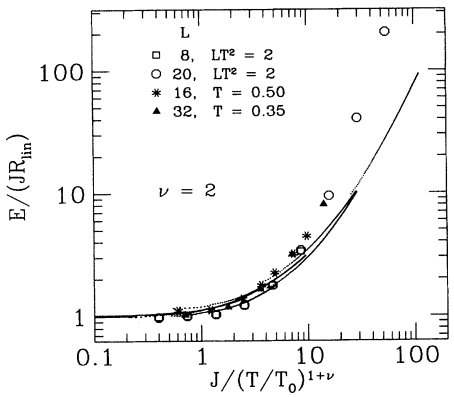

FIG. 10. Scaling plot combining the nonlinear current-voltage characteristics of both the experimental data in Fig. 1 (lines) and simulations (points). The data points with $LT^2 = 2$ were obtained from the random pinning potential model and the other two sets of data points, at $T = 0.35$ and 0.50, were obtained from the gauge glass in the vortex representation. The value $\nu = 2$ was used for all the data. The temperature scale was set by $T_0 = 1$ (random pinning potential model), $T_0 = 1.15$ (gauge glass), and $T_0 = 12$ K (experiment). The two sets of data from the simulations agree quite well with each other, but the experimental results lie lower than theory at large values of $J/T^{1+\nu}$.

is constant and $E/(JR_{\rm lin})$ should only be a function of J/T^3. The data is seen to scale very well over a wide range. These results provide strong evidence that the gauge-glass and random pinning potential models are in the same universality class with a correlation length exponent at the $T = 0$ transition of $\nu \simeq 2$.

Finally, in Fig. 10, we compare the nonlinear current-voltage characteristics from the simulations on the random pinning potential and gauge-glass models with the experimental results shown in Fig. 1. The same value of $\nu = 2$ was used for all the data, and, for each system, a temperature scale T_0 was adjusted to get the best scaling. The two sets of simulation data agree quite well with each other. While the gauge-glass data were obtained in the region where $\xi \ll L$, as deduced from the results for $R_{\rm lin}$, the random pinning potential model data were obtained in the finite-size region and so the data were taken at fixed LT^2 (or equivalently at fixed, but not very small, ξ/L). The good agreement between the two sets of data indicates that finite-size corrections are not very important for the I-V characteristics. There is, however, a small discrepancy between the numerical results and experiment at high currents, for which we do not have an explanation.

V. CONCLUSIONS

We have studied the I-V characteristics of two models for vortex-glass behavior in two dimensions. For the gauge glass, our results confirm earlier studies[6,8] which found a zero-temperature transition with a correlation length exponent $\nu \simeq 2$. This behavior has also been seen experimentally[12] on very thin films of Y-Ba-Cu-O, though the detailed form of the I-V scaling function is somewhat different between theory and experiment. We also find that the linear resistance varies with an Arrhenius form as the temperature approaches zero, indicating that the barrier exponent ψ is either zero or close to zero. Experimentally the resistance vanishes at low temperature less rapidly than an Arrhenius form, which may indicate that quantum fluctuations of the vortices play a role in the Y-Ba-Cu-O films. The random pinning potential model is more realistic in that it describes a system with a uniform applied magnetic field perpendicular to the film, as opposed to the gauge glass which has random fluxes. Nonetheless, the random pinning potential model is found to be in the same universality class as the gauge glass, since they both have a zero-temperature transition with $\nu \simeq 2$ and Arrhenius behavior for the linear resistance. Hence these two models are equivalent in two dimensions. It can also be shown that in $6-\epsilon$ dimensions, the gauge-glass transition is in the same universality class as the vortex-glass transition in a model with a spatially varying transition temperature and a net magnetic field. It is therefore quite plausible that the two models have the same critical behavior in three dimensions. We are not aware of a direct demonstration of this.

ACKNOWLEDGMENTS

We should like to thank C. Dekker for providing us with the data in Fig. 1. A.P.Y. is supported by NSF grants No. DMR 91-11576 and DMR-94-11964. M.P.A.F. is supported by NSF grants No. PHY89-04035 and DMR-9400142. S.M.G. and R.A.H. are supported by DOE Grant No. DE-FG02-90ER45427. M.W. is supported by the Swedish Natural Science Research Council.

[1] D. S. Fisher, M. P. A. Fisher, and D. A. Huse, Phys. Rev. B **43**, 130 (1991).
[2] See, e.g., K. B. Kim and M. J. Stephen, in *Superconductivity*, edited by R. D. Parks (Dekker, New York, 1969), Vol II.
[3] A. I. Larkin and Yu. N. Ovchinikov, J. Low. Temp. Phys. **34**, 409 (1979).
[4] M. P. A. Fisher, Phys. Rev. Lett. **62**, 1415 (1989).
[5] J. D. Reger, T. A. Tokuyasu, A. P. Young, and M. P. A. Fisher, Phys. Rev. B **44**, 7147 (1991).
[6] M. J. P. Gingras, Phys. Rev. B **45**, 7547 (1992); M. Cieplak, J. R. Banavar, and A. Khurana, J. Phys. A **24**, L145 (1991).
[7] R. H. Koch, V. Foglietti, W. J. Gallagher, G. Koren, A. Gupta, and M. P. A. Fisher, Phys. Rev. Lett. **63**, 1511 (1989); P. L. Gammel, L. F. Schneemeyer, and

D. J. Bishop, *ibid.* **66**, 953 (1991); C. Dekker, W. Eideloth, and R. H. Koch, *ibid.* **68**, 3347 (1992).
[8] M. P. A. Fisher, T. A. Tokuyasu, and A. P. Young, Phys. Rev. Lett. **66**, 2931 (1991).
[9] H. Nishimori, Physica A **205**, 1 (1994).
[10] H. S. Bokil and A. P. Young (unpublished).
[11] Y-H Li, Phys. Rev. Lett. **69**, 1819 (1992).
[12] C. Dekker, P. J. M. Wöltgens, R. H. Koch, B. W. Hussey, and A. Gupta, Phys. Rev. Lett. **69**, 2717 (1992).
[13] K. H. Lee and D. Stroud, Phys. Rev. B **43**, 5280 (1991).
[14] S. Shenoy, J. Phys. C **18**, 5163 (1985).
[15] K. K. Mon and S. Teitel, Phys. Rev. Lett. **62**, 673 (1989).
[16] J. Villain, J. Phys. (Paris) **36**, 581 (1975).
[17] J. V. José, L. P. Kadanoff, S. K. Kirkpatrick, and D. R. Nelson, Phys. Rev. B **16**, 1217 (1977); H. Kleinert, *Gauge Fields in Condensed Matter* (World Scientific, Singapore, 1989).
[18] M. Wallin and S. M. Girvin, Phys. Rev. B **47**, 14 642 (1993).
[19] A. P. Young, in *Proceedings of the Ray Orbach Inauguration Symposium* (World Scientific, Singapore, 1994).
[20] *Finite Size Scaling and Numerical Simulations of Statistical Systems*, edited by V. Privman (World Scientific, Singapore, 1990).
[21] Of course our numerical implementation of the continuous time dynamics uses a discrete time step, but this time step is much smaller than the characteristic microscopic time τ which corresponds to the time of one sweep in the Monte Carlo simulation.